Three-Dimensional Morphogeometric and Volumetric Characterization of Cornea in Pediatric Patients With Early Keratoconus

IBRAHIM TOPRAK, FRANCISCO CAVAS, JOSÉ S. VELÁZQUEZ, JORGE L. ALIÓ DEL BARRIO, AND JORGE L. ALIÓ

• PURPOSE: To present morphogeometric and volumetric characteristics of the cornea and its diagnostic value in pediatric patients with keratoconus (KC) using 3-dimensional (3-D) corneal modeling.

• DESIGN: Cross-sectional study.

• METHODS: This single-center (VISSUM Innovation, Alicante, Spain) study comprised 49 eyes of 49 pediatric patients (age ≤16 years) with KC and 31 eyes of 31 healthy pediatric controls. Eyes were graded as early (n = 21) and mild KC (n = 28) based on the RETICS (Thematic Network for Co-Operative Research in Health) classification system. The 3-D corneal model was generated using raw topographic data. Deviation of anterior ($D_{apexant}$) and posterior ($D_{apexpost}$) apex and minimum thickness points (D_{mctant}, $D_{mctpost}$), $D_{apexant}$-$D_{apexpost}$ difference, total corneal volume (V_{total}), volumetric distribution (VOL_{AAP}, VOL_{PAP}, and VOL_{MCT}), and percentage of relative volume increase (VOL_{AAPrel}, VOL_{PAPrel}, and VOL_{MCTrel}) between 2 consecutive radii centered to anterior/posterior apex and thinnest point were evaluated.

• RESULTS: $D_{apexpost}$ and $D_{apexant}$-$D_{apexpost}$ difference were higher in the early and mild KC groups compared to the control group ($P < .05$). Eyes with early and mild KC had decreased V_{total} compared with the control group ($P < .05$). $D_{apexpost}$, $D_{apexant}$-$D_{apexpost}$ difference, and VOL_{MCTrel} between 1.0 and 1.4 mm diameters had area under receiver operating characteristics curve (AUROC) values over 0.93 in discrimination of early KC from normal.

• CONCLUSIONS: This is the first study presenting morphogeometric and volumetric characterization of cornea in pediatric patients with early and mild KC using a 3-D corneal model. Integration of the morphogeometric and volumetric parameters to topography software can add value in early detection of KC in pediatric patients. (Am J Ophthalmol 2021;222:102–111. © 2020 Elsevier Inc. All rights reserved.)

KERATOCONUS (KC) IS A MULTIFACTORIAL, PROgressive, and asymmetric disorder associated with corneal biomechanical instability. KC typically manifests in the second decade of life; however, current literature points to puberty as the starting point.[1,2] On the other hand, manifestation of KC was reported as early as 4 years of age.[3]

Current scientific data conclude that pediatric cases of KC tend to progress more rapidly and the need for corneal transplantation is 7-fold higher.[4] This condition has been suggested to be originated from differences in structural and biomechanical properties of the cornea between the pediatric and adult population.[4,5] For instance, the pediatric cornea is more elastic and intrastromal collagen turnover is faster. In pediatric KC, weak collagen lamellae cannot be properly compensated by the age-related natural stiffening process. Therefore, younger KC patients tend to show more aggressive progression.[4,5] It was previously shown that cone is more centrally located in pediatric patients and the disease is more advanced at the time of diagnosis.[4–6] Current literature has evidence that there are differences regarding viscoelastic and biomechanical properties of the cornea when compared to the adult patients.[4–6] However, it has not been fully clarified whether these particular differences might affect 3-dimensional (3-D) morphogeometric and volumetric characterization of pediatric cornea with KC.

In recent years, studies by Cavas-Martinez and associates[7–9] introduced an innovative 3-D solid model of normal and keratoconic cornea and various novel indices, which allow quantitative assessment of morphogeometric and volumetric properties of the cornea.[7–9] This study aims to represent morphogeometric and volumetric features of the cornea and their diagnostic role in pediatric patients (≤16 years of age) with early KC using 3-D corneal modeling.

Accepted for publication Sep 14, 2020.

From the Department of Ophthalmology, Faculty of Medicine, Pamukkale University, Denizli, Turkey (I.T.); Department of Research and Development (I.T., J.L.A.B., J.L.A.), VISSUM, Alicante, Spain; Department of Structures, Construction and Graphical Expression, Technical University of Cartagena, Cartagena, Spain (F.C., J.S.V.); Cornea, Cataract and Refractive Surgery Department (J.L.A.B., J.L.A.), VISSUM, Alicante, Spain; and Division of Ophthalmology, Department of Pathology and Surgery, Faculty of Medicine, Miguel Hernández University, Alicante, Spain (J.L.A.B., J.L.A.).

Inquiries to Jorge L. Alió, VISSUM, Cornea, Cataract and Refractive Surgery Unit and Division of Ophthalmology, Department of Pathology and Surgery, Faculty of Medicine, Miguel Hernández University, Calle Cabañal, 1, Edificio Vissum, 03016 Alicante, Spain; e-mail: jlalio@vissum.com

0002-9394/$36.00
https://doi.org/10.1016/j.ajo.2020.09.031

METHODS

THIS CROSS-SECTIONAL STUDY FOLLOWED THE TENETS OF Declaration of Helsinki on the use of human subjects in research, and institutional ethics committee approval was obtained.

• **STUDY POPULATION:** The study comprised 49 eyes of 49 pediatric patients (≤16 years of age) with a confirmed diagnosis of KC and 31 eyes of 31 healthy pediatric controls with normal corneal topography (provided from VISSUM Innovation, Cornea, Cataract and Refractive Surgery Unit, Alicante, Spain, which is also affiliated with Miguel Hernandez University and the Keratoconus IBERIA database).

Keratoconus group. A single experienced cornea specialist (J.L.A.) verified the diagnosis of KC in each case based on the combination of the following findings: presence of typical topographic patterns for KC on axial curvature map (round, oval, superior steep, inferior steep, irregular, inferior-steep asymmetric bowtie, superior-steep asymmetric bowtie, and symmetric or asymmetric bowtie with skewed radial axes >21°); central/paracentral or inferior focal steepening (anterior and/or posterior) and/or corneal thinning; 3-mm inferior-superior (I-S) mean keratometric difference >1.4 diopters (D).[10,11] Eyes were graded regarding disease severity based on the RETICS (Thematic Network for Co-Operative Research in Health) KC classification system.[12] Twenty-one eyes had *early KC* (grade 1) based on the following criteria: spectacle-corrected distance visual acuity (CDVA) >0.9 Snellen equivalent, central K <46.5 D, coma-like aberration root mean square (RMS) <2.5 μm, 8-mm Q-value <-0.35 μm, and internal astigmatism <2.5 D. On the other hand, 28 eyes were classified as mild (grade 2 and grade 3) KC (CDVA = 0.4-0.9 Snellen equivalent, central K = 46.5-53 D, coma-like aberration RMS = 2.5-4.5 μm, 8-mm Q-value between -0.35 and -1.10 μm, and internal astigmatism = 2.5-4.5 D).[12]

The RETICS KC classification system was previously introduced by Alió and associates and validated by further studies.[12–14]

Control group. The control pediatric group included randomly selected (IBM SPSS Statistics Inc, Chicago, Illinois, USA) 1 eye of 31 subjects with normal clinical examination and normal topography. None of the subjects showed above-mentioned abnormal findings and all had a CDVA ≥1.0 Snellen equivalent.

Poor compliance to topography measurements, low test quality, previous history of anterior segment surgery, corneal scarring, infection, and any corneal thinning disorders were accepted as the exclusion criteria.

Validation group. A pediatric (age ≤16 years) Down syndrome (DS) group (9 eyes had early KC and 3 eyes were normal) was included in the current study to test the ability of 3-D morphogeometric/volumetric parameters for detecting early KC.

• **EXAMINATION AND MEASUREMENTS:** All subjects underwent ophthalmologic examinations including CDVA assessment, slit-lamp biomicroscopy, dilated fundus examination, and retinoscopy. Participants were requested to remove their contact lenses prior to the measurements for at least 2 weeks (for soft contact lenses) or 3 weeks (for hard contact lenses). A single experienced optometrist performed at least 3 topography measurements (Sirius System; CSO, Florence, Italy) for each eye. Test with the best image acquisition quality (coverage and centration scores >90%) with a green-colored checkmark were used for the statistical analysis.

Spherical equivalent values; RMS values for high-order, coma, spherical, and total aberrations; Q-value (8 mm); minimum corneal thickness (MCT), and central corneal thickness measurements obtained from the topographer were noted.

Apart from this, the whole set of corneal tomographies was exported in.CSV format, in order to be subsequently analyzed in detail by means of a biometric characterization procedure developed and validated by our research group.[7–9]

• **MORPHOGEOMETRIC CHARACTERIZATION:** The morphogeometric characterization procedure applied in this research work was built over the following phases (Figure 1):

(1) Generation of the point cloud. We used a 3-D spatial coordinate system for the generation of the surface that fits the cloud of points. We used a self-developed algorithm, programmed in the commercial software MATLAB R2018b (MathWorks, Natick, Massachusetts, USA), to change to Cartesian format the coordinates contained in each topographic file, before they are exported in.CSV format. Each row represents a circle depicted over the corneal map, and each column represents a semi-meridian (256 points taken per each radius). Rows samples are taken in a circular trajectory of radius i*0.2 mm, "i" being the row number, and column samples are taken following a semi-meridian in the path of j*360/256u, "j" being the column number.

At last, a matrix with the format [i, j] was created, in which each Z value characterizes the point P (i*0.2, j*360/256u) in polar coordinates. Using this arrangement,

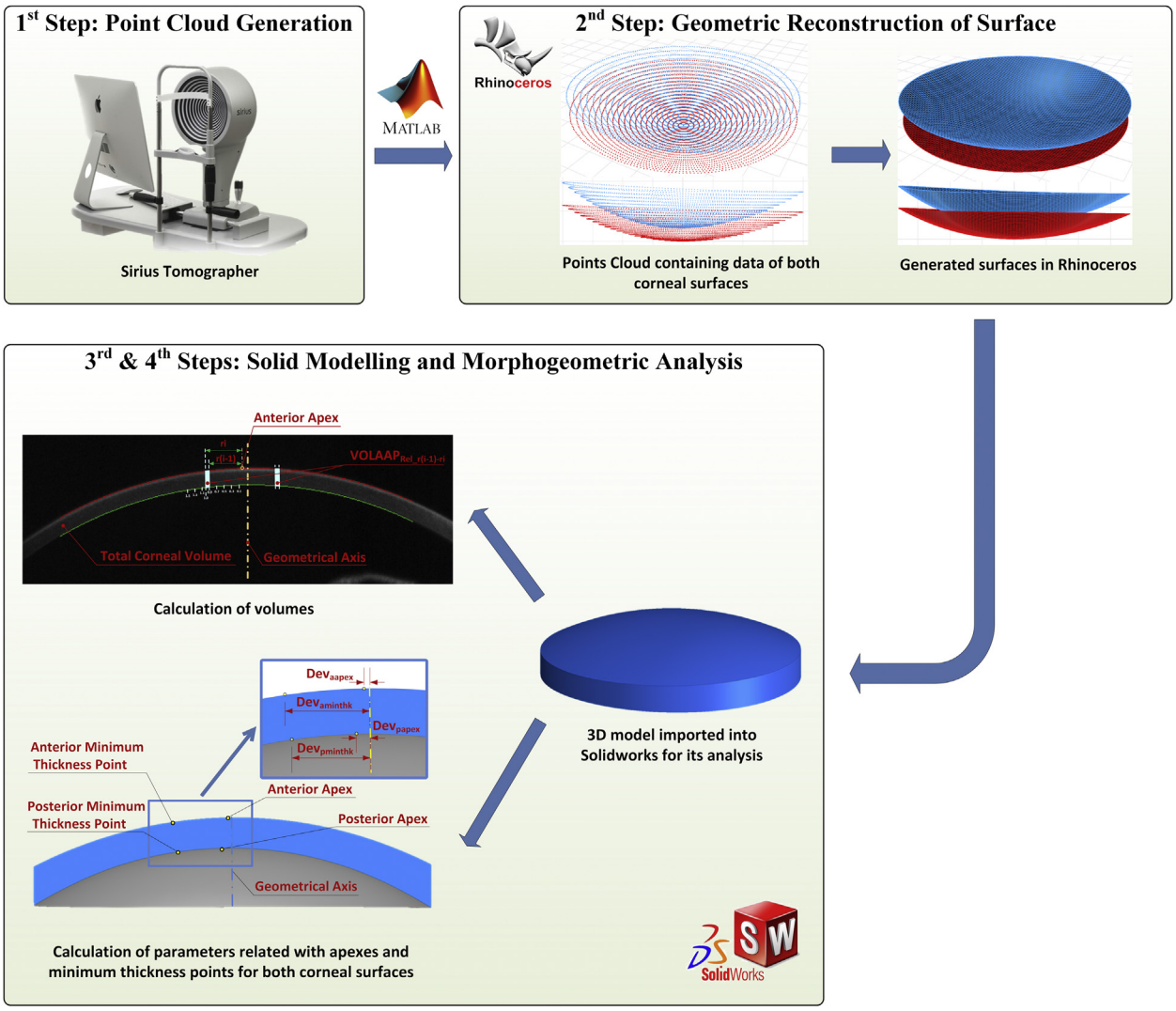

FIGURE 1. The 4 steps that conform the morphogeometric characterization procedure.

a point cloud was created for the area that extends from the geometric center of the cornea (r = 0 mm) to the mid-peripheral area (r = 4 mm). This area of study usually contains most information about corneal biometry for both healthy and diseased eyes.[7]

(2) Corneal surface reconstruction. The point cloud representing the corneal biometry was then exported to the 3-D surface reconstruction software Rhinoceros V 5.0 (McNeel & Associates, Seattle, Washington, USA). In order to optimize the fitting between the point cloud and the surface generated, we made use of Rhinoceros patch surface functionality to minimize the spatial separation between the 3-D point cloud and the produced surface. The configuration settings fixed for the function were as follows: sample point spacing: 256; surface span planes: 255 for both "u" and "v" directions; stiffness of the solution surface: 1.

(3) 3-D custom modeling. The surface generated in preceding stages was then exported to the solid modeling software SolidWorks V2018 (Dassault Systèmes, Vélizy-Villacoublay, France). By means of this software, the 3-D custom model representing the corneal biometry was generated.[7]

(4) Morphogeometric variables calculation. Most of these variables and the way they are calculated have already been exhaustively described in prior research by our group.[7–9] Similarly, this study uses several volumetric parameters directly related with volumes around anterior and posterior apices and minimum thickness points, which have also been successfully used in previous researches for keratoconus diagnosis,[8] but to the authors' knowledge this is the first time they are used for pediatric keratoconus characterization. In addition, 3 new morphogeometric variables were defined, the percentage of relative volume increase between 2

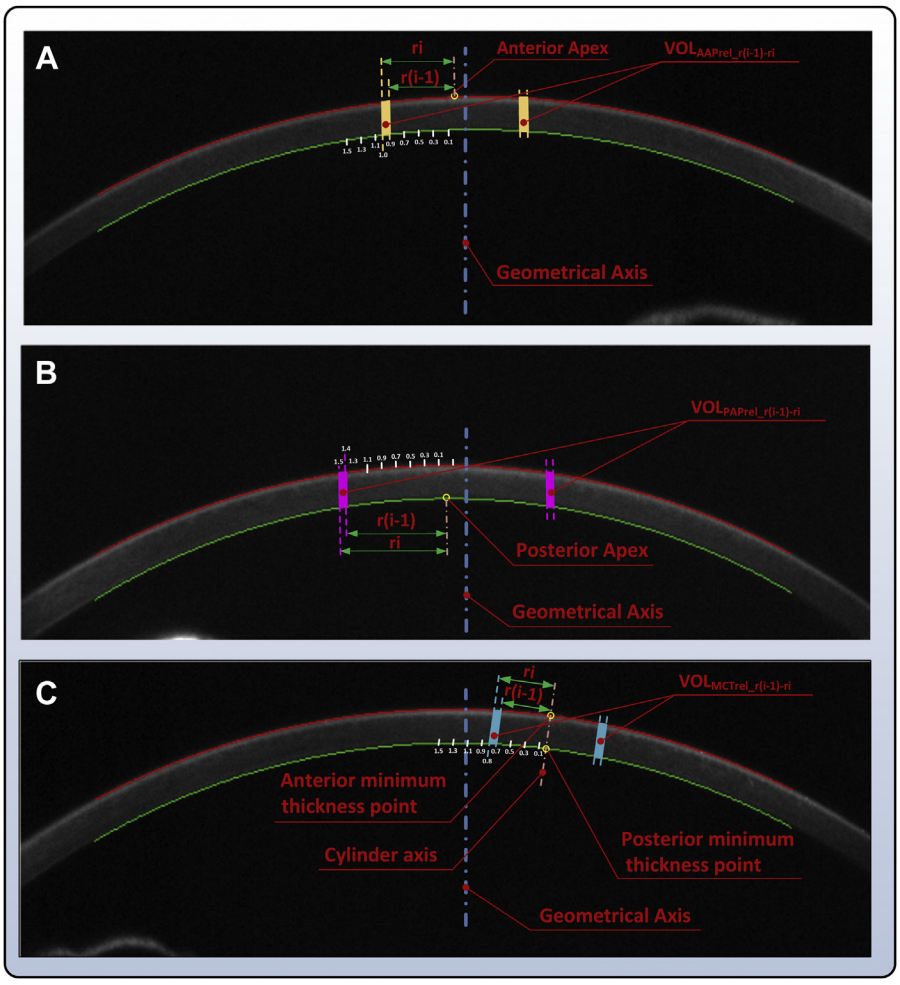

FIGURE 2. Definition of the new relative volume increase between 2 consecutive radii variables, for anterior apex (VOL_{AAPrel}) (panel A), posterior apex (VOL_{PAPrel}) (panel B), and minimum corneal thickness (VOL_{MCTrel}) points (panel C).

consecutive radii, "i" being each radius step ri = 0.2, …,1.5, starting at r = 0.1, centered around anterior apex (AAP), posterior apex (PAP), and MCT points (Figure 2). All proposed morphogeometric parameters are summarized in Table 1.

• **STATISTICAL ANALYSIS:** Assuming an effect size (d) of 0.8, 39 patients with KC and 31 control subjects (a total of 70 subjects) provided 95% power at 95% confidence level (G*Power version 3.1.9.2 computer software; Universität Düsseldorf, Düsseldorf, Germany).

Statistical Package for Social Sciences (SPSS) version 24 (IBM SPSS Statistics Inc, Chicago, Illinois, USA) software was used for statistical analysis. Categorical data (sex) were analyzed using the χ^2 test. Quantitative variables (age, refractive, topographic, morphogeometric and volumetric measurements) were expressed as mean ± standard deviation (SD). A Kruskal-Wallis H test was performed to compare quantitative variables among the control, early KC, and mild KC groups initially ($P < .05$ indicated statistical significance). For post hoc corrections, the Mann-Whitney *U* test was used for pairwise comparisons (control vs early KC, control vs mild KC, and early vs mild KC) and statistical significance level was set at $P < .0166$.

Diagnostic performance of the variables was tested using receiver operating characteristic (ROC) analysis. Area under the ROC curve (AUC) was calculated to test the ability of these variables on discrimination of early KC from healthy pediatric controls. AUC values were classified as follows: excellent (0.90-1.00), good (0.80-0.89), fair (0.70-0.79), poor (0.60-0.69), and worthless (0.50-0.59). An ROC curve plots true-positive rate (sensitivity) against the false-positive rate (1 − specificity) for different threshold values, and values with the best sensitivity-specificity pair on the ROC curve were accepted as the threshold. Sensitivity was defined as (true positives)/(true positives + false negatives) ratio, while the specificity indicated the ratio of (true negatives)/(true negatives + false positives). A multivariate logistic regression analysis was

TABLE 1. Morphogeometric and Volumetric Indices Proposed for Pediatric Keratoconus Characterization

Morphogeometric Parameter	Acronym
Anterior and posterior apex deviation (mm)	$D_{apexant}/D_{apexpost}$
Anterior and posterior minimum thickness point deviation (mm)	$D_{mctant}/D_{mctpost}$
Anterior/posterior corneal surface area (mm^2)	A_{ant}/A_{post}
Total corneal surface area (mm^2)	A_{tot}
Anterior/posterior sagittal plane apex area([mm^2)	$A_{apexant}/A_{apexpost}$
Sagittal plane area in posterior minimum thickness point (mm^2)	$A_{mctpost}$
Total corneal volume (mm^3)	V_{total}
Corneal volume R-x defined by the points of minimal thickness (mm^3)	Vol_{MCT}
Corneal volume R-x defined by the anterior corneal apex (mm^3)	Vol_{AAP}
Corneal volume R-x defined by the posterior corneal apex (mm^3)	Vol_{PAP}
Relative volume increase between 2 consecutive radii (ri = 0.2, …,1.5), starting at r = 0.1, centered around anterior apex (%)	$VOL_{AAPrel\_r(i-1)-ri}$
Relative volume increase between 2 consecutive radii (ri = 0.2, …,1.5), starting at r = 0.1, centered around posterior apex (%)	$VOL_{PAPrel\_r(i-1)-ri}$
Relative volume increase between 2 consecutive radii (ri = 0.2, …,1.5), starting at r = 0.1, centered around minimum thickness point (%)	$VOL_{MCTrel\_r(i-1)-ri}$

also performed to predict influence of multiple variables on having early KC. A P value <.05 was accepted as statistically significant at 95% confidence interval.

The main outcome measures were defined as spherical equivalent value; RMS values for high-order, coma, spherical, and total aberrations; Q-value (for 8 mm); central and minimum corneal thicknesses; $D_{apexant}$; $D_{apexpost}$; D_{mctant}; $D_{mctpost}$; A_{ant}; A_{post}; A_{tot}; $A_{apexant}$; $A_{apexpost}$; $A_{mctpost}$; $D_{apexant}$-$D_{apexpost}$ difference; VOL_{total}; VOL_{MCT}; VOL_{AAP}; VOL_{PAP}; VOL_{MCTrel}; VOL_{AAPrel}; and VOL_{PAPrel} (Table 1).

RESULTS

TABLE 2 REPRESENTS COMPARISON OF AGE; SPHERICAL equivalent value; RMS values for high-order, coma, spherical, and total aberrations; Q-value (for 8 mm); and central and minimum corneal thicknesses among the control, early KC, and mild KC groups.

• **MORPHOGEOMETRIC PARAMETERS:** The mild pediatric KC group had significantly higher $D_{apexant}$, $A_{apexant}$, A_{ant}, and A_{post} values than in the early KC and control groups (Table 3, $P < .05$). $D_{apexpost}$ was significantly higher in both early and mild KC groups when compared to the control group. However, in both KC groups, $A_{apexpost}$ and $A_{mctpost}$ values were found significantly reduced compared with the control group (Table 3, $P < .05$). $D_{apexant}$-$D_{apexpost}$ difference was also calculated and was significantly higher (absolute value) in both KC groups compared with the control group (Table 3, $P < .05$). Table 3 shows comparative morphogeometric data between the groups.

• **VOLUMETRIC PARAMETERS:** Total corneal volume (V_{total}) was significantly reduced in the early and mild KC groups (24.0 ± 1.7 mm^3 and 24.3 ± 1.8 mm^3, respectively) compared with the control group (25.9 ± 1.4 mm^3) ($P < .0001$). Similarly, VOL_{MCT}, VOL_{AAP}, and VOL_{PAP} (for each 0.05-mm step of the radius value, within 0.1-1.5 mm diameter) values were also lower in the early and mild KC groups compared to those of the control group ($P < .001$) (Figure 3).

There were significant differences between the control vs mild KC and early vs mild KC groups regarding percentage of relative volume increase (PRVI) between 2 consecutive radii (with 0.05-mm steps, which equals 0.1 mm of diameter steps) centered on the MCT (VOL_{MCTrel}) beginning from 0.3 mm of diameter up to 1.1 mm; and between 1.3 and 1.5 mm (Figure 4). However, between 1.1 and 1.3 mm of diameter ($VOL_{MCTrel1.1\text{-}1.2}$ and $VOL_{MCTrel1.2\text{-}1.3}$), significant differences were detected between the control vs early KC, control vs mild KC, and early vs mild KC groups (Figure 4).

On the other hand, regarding PRVI between 2 consecutive radii (with 0.05-mm steps) centered according to the anterior and posterior corneal apices (VOL_{AAPrel} and VOL_{PAPrel}), statistically significant differences were detected between the control vs mild KC and early vs mild KC groups beginning from 0.5 mm up to 1.5 mm of the diameter values (Figure 4). Figure 4 presents graphical comparison of PRVI values between 2 consecutive radii emerging from thinnest corneal point, anterior apex, and posterior apex (VOL_{MCTrel}, VOL_{AAPrel}, and VOL_{PAPrel}, respectively).

• **DIAGNOSTIC VALUE OF THE VARIABLES:** The ROC analysis showed that $VOL_{MCTrel1.3\text{-}1.4}$ (AUC = 0.965, $P < .0001$, 95.2% sensitivity and 83.9% specificity), $D_{apexpost}$ (AUC = 0.947, $P < .0001$, 81% sensitivity and 100% specificity), $D_{apexant}$-$D_{apexpost}$ difference (AUC = 0.947, $P <$

TABLE 2. Comparison of Age, Spherical Equivalent Value, Corneal Aberrations, and Pachymetry Among the Control Group and Early and Mild Pediatric Keratoconus Groups

	Groups				
	Control Group (N = 31)	Early KC (N = 21)	Mild KC (N = 28)	*P* Value[a]	*P* Value[b]
Age (years)	12.8 ± 2.5	13.9 ± 1.5	14.0 ± 1.6	.166	–
Spherical equivalent (diopters)	−3.14 ± 4.05	−0.88 ± 1.40	−4.63 ± 4.16	**.0001**	**.002**[e]
RMS-HOA (μm)	0.37 ± 0.09	1.27 ± 0.71	3.05 ± 2.0	**.0001**	**.0001**[c,d,e]
RMS-coma (μm)	0.24 ± 0.12	0.93 ± 0.58	2.69 ± 1.92	**.0001**	**.0001**[c,d,e]
RMS-spherical aberration (μm)	0.20 ± 0.04	0.18 ± 0.23	−0.33 ± 0.83	**.0001**	**.0001, .002**[d,e]
Total RMS (μm)	0.93 ± 0.47	2.38 ± 1.34	4.83 ± 2.62	**.0001**	**.012, .0001, .000**[c,d,e]
Q-value 8 mm (μm)	−0.13 ± 0.15	−0.34 ± 0.36	−1.16 ± 0.62	**.0001**	**.0001**[d,e]
Minimum corneal thickness (μm)	540.5 ± 29.1	486.7 ± 43.0	459.0 ± 63.6	**.0001**	**.0001**[c,d]
Central corneal thickness (μm)	543.6 ± 29.1	517.4 ± 22.4	475.6 ± 55.9	**.0001**	**.0001, .001**[d,e]

HOA = high-order aberrations; KC = keratoconus; RMS = root mean square.

All quantitative values are given as mean ± standard deviation. Bold values indicate statistical significance between the groups ($P < .05$ or $P < .0166$).

[a]*P* values for comparison of the control, early keratoconus, and mild keratoconus groups (Kruskal-Wallis test; $P < .05$ indicates statistically significant difference).

[b]*P* values for pairwise comparisons (footnotes c, d, e) with post hoc corrections.

[c]Statistically significant difference between the control and early KC groups ($P < .0166$ indicates statistically significant difference after Bonferroni correction).

[d]Statistically significant difference between the control and mild KC groups ($P < .0166$ indicates statistically significant difference after Bonferroni correction).

[e]Statistically significant difference between the early KC and mild KC groups ($P < .0166$ indicates statistically significant difference after Bonferroni correction).

.0001, 81% sensitivity and 100% specificity), $VOL_{MCTrel1.0\text{-}1.1}$ (AUC = 0.939, $P < .0001$, 95.2% sensitivity and 77.4% specificity), $VOL_{MCTrel1.1\text{-}1.2}$ (AUC = 0.937, $P < .0001$, 90.5% sensitivity and 80.6% specificity), and $VOL_{MCTrel1.2\text{-}1.3}$ (AUC = 0.937, $P < .0001$, 90.5% sensitivity and 83.9% specificity) had the highest AUC values (in order) for distinguishing eyes with early KC from normal. Figure 5 shows AUC graphs for these variables.

Logistic regression analyses were performed; created statistically significant ($P < .05$) multifactorial models did not show better diagnostic ability (AUC values <0.900) than any individual above-mentioned variables in detection of early KC.

• **VALIDATION GROUP ANALYSIS:** In the DS group, it was found that $D_{apexant}$ (AUC= 0.938, $P < .0001$, 100% sensitivity and 88.2% specificity) and V_{total} (AUC = 0.928, $P < .0001$, 100% sensitivity and 85.3% specificity) had excellent sensitivity and good specificity for distinguishing early KC from normal. However, $D_{apexpost}$, $D_{apexant}$-$D_{apexpost}$ difference, and PRVI centered to thinnest point (VOL_{MCTrel}) failed to give significant AUC values (AUC <0.600, $P > .05$).

DISCUSSION

THIS IS THE FIRST CLINICAL STUDY PRESENTING MORPHOgeometric and volumetric characteristics of the cornea based on a 3-D virtual model and its diagnostic value in pediatric patients with early and mild KC. The current study demonstrated significant differences between eyes with early and mild KC regarding deviation in corneal apex. For instance, anterior corneal apex was more displaced from corneal vertex ($D_{apexant}$) in the mild KC group when compared to the control and early KC groups, while deviation in anterior apex did not differ between early KC and healthy controls. On the other hand, deviation of the posterior apex ($D_{apexpost}$) and difference between anterior and posterior apex deviation ($D_{apexant}$-$D_{apexpost}$) (absolute value) were significantly higher in the early and mild KC groups than in the control group. Significant deviation of the apical points in the KC groups indicates abnormal conical formation that lead change in apex location. Furthermore, these findings also reveal that in earlier stages of KC, the posterior apex starts to displace first (early KC); and once the disease continues advancing, anterior apex displacement becomes evident (mild KC). From a diagnostic perspective, deviation in posterior apex and asymmetry between anterior and posterior apex deviation seem to have excellent specificity and modest sensitivity for distinguishing early KC from normal in a pediatric population (with 81% sensitivity and 100% specificity).

Interestingly, deviation of the MCT (D_{mctant} and $D_{mctpost}$) did not differ among the 3 groups. The floppy and unstable nature of the pediatric cornea (in contrast to adult cornea) might lead to a similar amount of MCT displacement in the control and KC groups.[2,15–17]

TABLE 3. Comparison of Morphogeometric Parameters Between the Control Group and Early and Mild Pediatric Keratoconus Groups

Parameter	Control Group (N = 31)	Early KC Group (N = 21)	Mild KC Group (N = 28)	P^a	P^b
$D_{apexant}$ (mm)	0.00006 ± 0.0003	0.0004 ± 0.0012	0.01689 ± 0.0177	<.0001*	<.0001*[d,e]
$D_{apexpost}$ (mm)	0.0631 ± 0.0195	0.1670 ± 0.0913	0.1757 ± 0.1054	<.0001*	<.0001*[c,d]
D_{mctant} (mm)	0.8862 ± 0.2583	1.0936 ± 0.3891	0.9133 ± 0.4264	.114	–
$D_{mctpost}$ (mm)	0.8136 ± 0.2469	1.0240 ± 0.3763	0.8479 ± 0.4055	.111	–
A_{ant} (mm^2)	43.11 ± 0.11	43.13 ± 0.19	43.51 ± 0.44	<.0001*	<.0001*[d,e]
A_{post} (mm^2)	44.38 ± 0.24	44.34 ± 0.31	44.91 ± 0.72	.001*	<.0001*[d,e]
A_{tot} (mm^2)	104.37 ± 1.16	103.23 ± 1.25	104.48 ± 1.59	.004*	.012,* 0.006*[c,e]
$A_{apexant}$ (mm^2)	0.14 ± 0.82	0.56 ± 1.42	3.43 ± 1.45	<.0001*	<.0001*[d,e]
$A_{apexpost}$ (mm^2)	4.34 ± 0.23	4.00 ± 0.32	4.02 ± 0.33	<.0001*	<.0001*[c,d]
$A_{mctpost}$ (mm^2)	4.33 ± 0.23	4.00 ± 0.32	4.00 ± 0.33	<.0001*	<.0001,* .001*[c,d]
$D_{apexant}$-$D_{apexpost}$ difference (mm)	−0.06 ± 0.01	−0.16 ± 0.09	−0.15 ± 0.10	<.0001*	<.0001*[c,d]

KC = keratoconus.

All quantitative values are given as mean ± standard deviation (SD).

$P < .05$ or $P < .0166$ (denoted by an asterisk) indicates statistical significance.

Parameters are defined as follows:

$D_{apexant}$ and $D_{apexpost}$: Average distance from the Z axis to the highest point (apex) of the anterior and posterior corneal surfaces, respectively.

D_{mctant} and $D_{mctpost}$: Average distance in the XY plane from the Z axis to the minimum thickness points of the anterior and posterior corneal surfaces, respectively.

A_{ant} and A_{post}: Area of the anterior and posterior corneal surfaces.

A_{tot}: Sum of anterior, posterior, and perimetric corneal surface areas.

$A_{apexant}$ and $A_{apexpost}$: Sagittal plane apex area of the cornea within the sagittal plane passing through the Z axis and the highest point (apex) of the anterior and posterior corneal surfaces.

$A_{mctppost}$: Sagittal plane area of the cornea within the sagittal plane passing through the Z axis and the minimum thickness points in the posterior corneal surface.

[a]*P* values for comparison of the control, early keratoconus, and mild keratoconus groups (Kruskal-Wallis test; $P < .05$ indicates statistically significant difference).

[b]*P* values for pairwise comparisons (footnotes c, d, e) with post hoc corrections

[c]Statistically significant difference between the control and early KC groups ($P < .0166$ indicates statistically significant difference after Bonferroni correction).

[d]Statistically significant difference between the control and mild KC groups ($P < .0166$ indicates statistically significant difference after Bonferroni correction).

[e]Statistically significant difference between the early and mild KC groups ($P < .0166$ indicates statistically significant difference after Bonferroni correction).

Increased anterior and posterior surface area (A_{ant} and A_{post}) in eyes with KC compared to eyes in the control group might indicate presence of focal elevations in anterior and posterior cornea, which lead increase in the surface area. Posterior sagittal plane areas for apex and MCT ($A_{apexpost}$ and $A_{mctpost}$) were significantly lower in the early and mild KC groups than in the control group. This finding might be owing to decreased corneal thickness values in eyes with KC, because thinner cornea lowers sagittal surface area value.

Volumetric analysis showed that total corneal volume and corneal volume for each 0.05 mm of radius value (diameter steps of 0.1 mm) of the revolution cylinder (up to 1.5 mm) centered according to MCT, anterior apex, and posterior apex were reduced in the early and mild KC groups compared to the controls. Corneal thinning (which was also topographically evident) is the most probable reason for decrease in corneal volume parameters in eyes with KC. Furthermore, the present study also evaluated PRVI between 2 consecutive radii (with 0.05 mm steps) centered to MCT and anterior and posterior corneal apices. Significant differences in PRVI were detected between the control vs mild KC and early vs mild KC groups beginning from the 0.3 and 0.5 mm of the diameter values when MCT and corneal apex (both anterior and posterior) were accepted as the center. When the control and early KC groups were compared, significant differences were only detected between 1.1 and 1.3 mm ($VOL_{MCTrel1.1\text{-}1.2}$ and $VOL_{MCTrel1.2\text{-}1.3}$) of the diameter values around the MCT regarding PRVI. Similarly, ROC analyses showed that PRVI between 1.0 and 1.3 mm of diameter values ($VOL_{MCTrel1.0\text{-}1.1}$, $VOL_{MCTrel1.1\text{-}1.2}$, and $VOL_{MCTrel1.2\text{-}1.3}$) around MCT had >90% sensitivity and >77% specificity in detection of early KC. More importantly, between 1.3

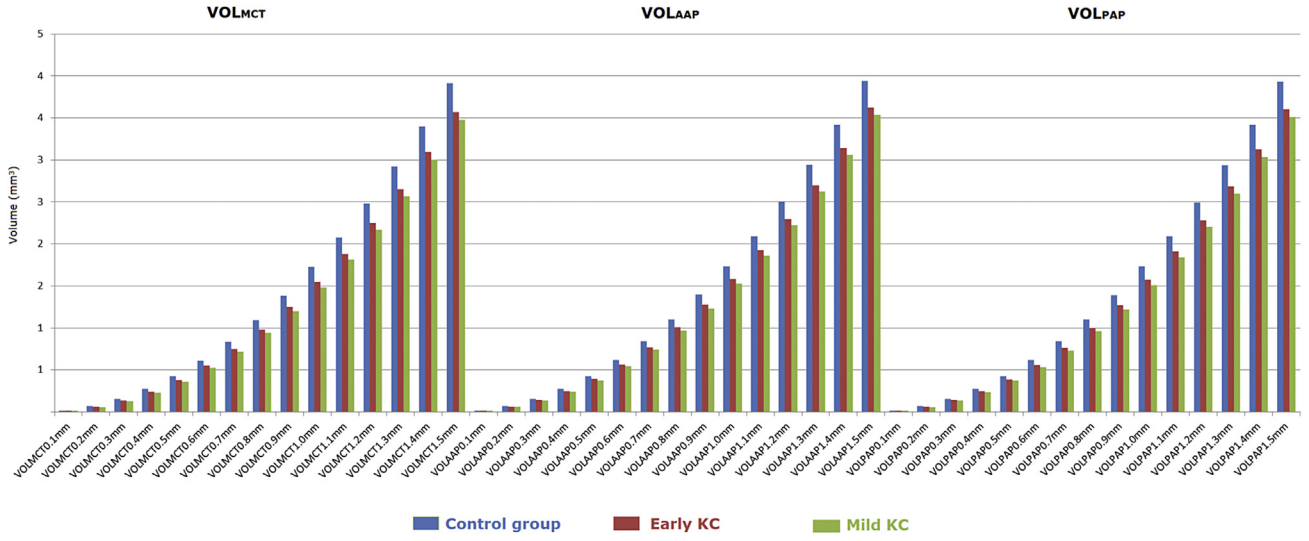

FIGURE 3. Corneal volume was significantly reduced in the early and mild keratoconus group for each 0.05-mm step of the radius value (diameter from 0.1 to 1.5 mm), in which axis was defined by a straight line perpendicular to tangent plane to minimum corneal thickness (VOL_{MCT}), anterior apex (VOL_{AAP}), and posterior apex (VOL_{PAP}). KC = keratoconus.

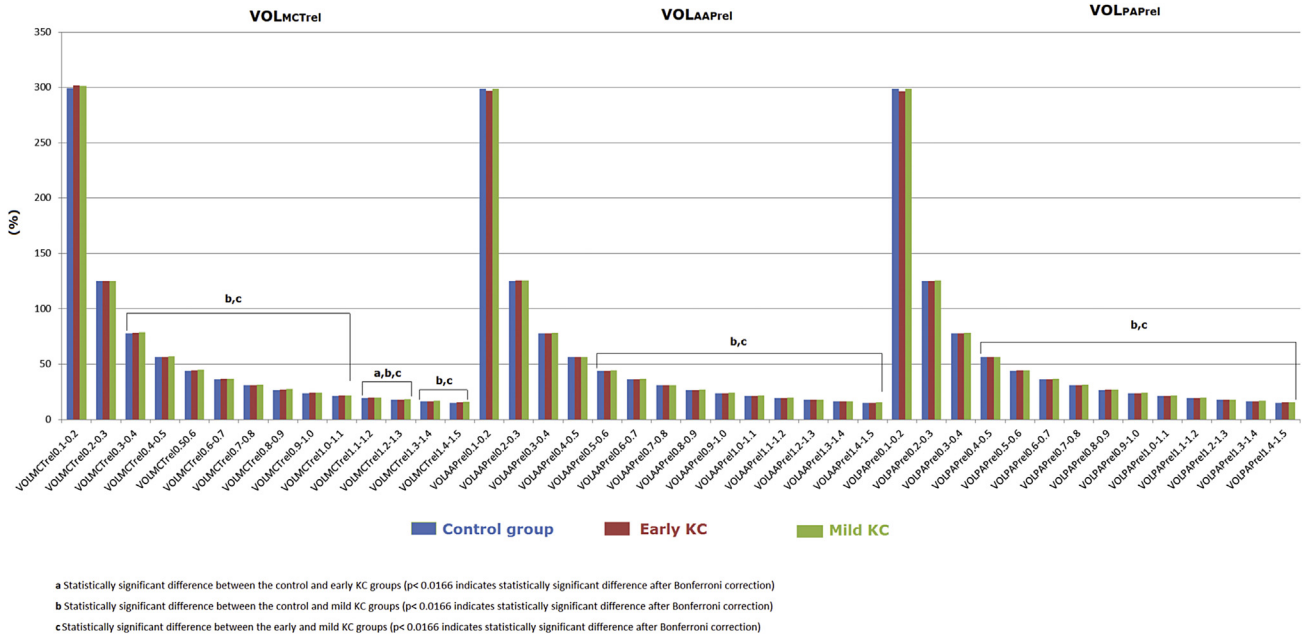

FIGURE 4. Comparative graph showing percentage of relative volume increase between 2 consecutive radii, "i" being each radius step r_i = 0.2, …,1.5, starting at r = 0.1, centered around minimum corneal thickness (VOL_{MCTrel}), anterior apex (VOL_{AAPrel}), and posterior apex (VOLPAPrel). KC = keratoconus.

and 1.4 mm of diameter, PRVI ($VOL_{MCTrel1.3\text{-}1.4}$) reached 95.2% sensitivity and 83.9% specificity in detection of early KC. We suggest that PRVI between 1.0 and 1.4 mm of diameter around the thinnest point (MCT) appear to have satisfying ability to detect early KC. This condition might be related to abrupt change in corneal thickness at this area.

Corneal thickness and volume distribution profiles were previously presented by Ambrosio and associates,[18] and they found significant alterations in corneal thickness spatial profile, corneal volume distribution, percentage increase in thickness, and percentage increase in volume in eyes with KC. They performed calculations within diameters from 1.0 to 7.0 mm with 0.25 mm of radius intervals

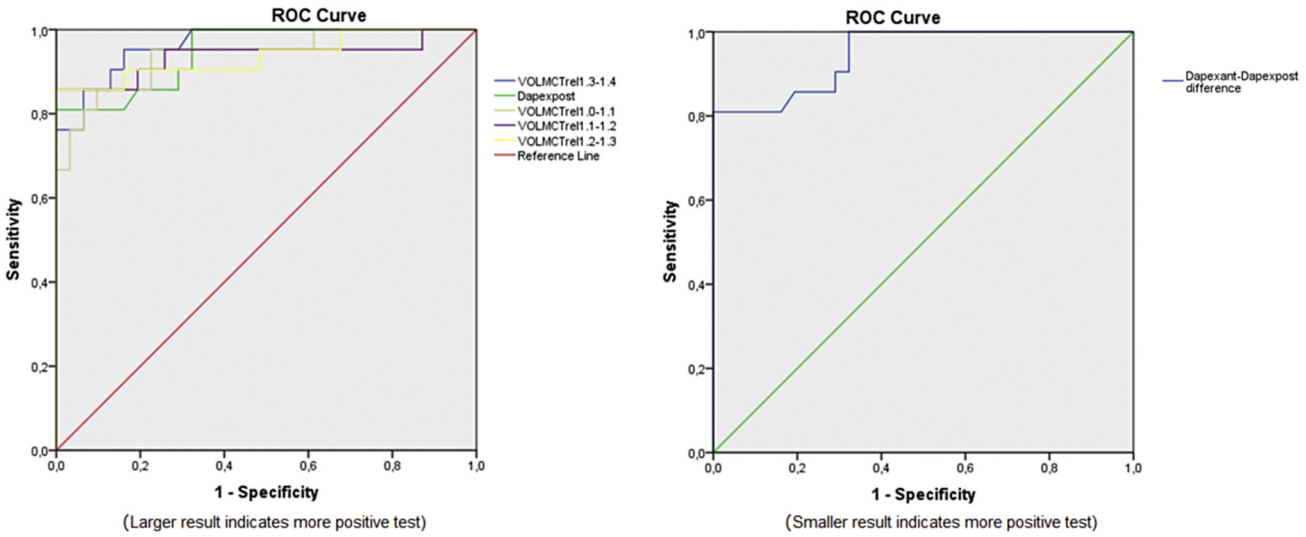

FIGURE 5. Receiver operating characteristic (ROC) curves showing sensitivity and 1 – specificity values for $VOL_{MCTrel1.3\text{-}1.4}$ (area under the curve [AUC] = 0.965, $P < .0001$, 95.2% sensitivity and 83.9% specificity), $D_{apexpost}$ (AUC = 0.947, $P < .0001$, 81% sensitivity and 100% specificity), $D_{apexant}$-$D_{apexpost}$ difference (AUC = 0.947, $P < .0001$, 81% sensitivity and 100% specificity), $VOL_{MCTrel1.0\text{-}1.1}$ (AUC = 0.939, $P < .0001$, 95.2% sensitivity and 77.4% specificity), $VOL_{MCTrel1.1\text{-}1.2}$ (AUC = 0.937, $P < .0001$, 90.5% sensitivity and 80.6% specificity), and $VOL_{MCTrel1.2\text{-}1.3}$ (AUC = 0.937, $P < .0001$, 90.5% sensitivity and 83.9% specificity) in discrimination of early keratoconus from normal in pediatric group.

centered on MCT. In the current study, we used 0.05 mm of radius steps for calculations, which could be more sensitive to any volumetric change when compared to the analysis by Ambrosio and associates.[18] Furthermore, corneal volume distribution and PRVI were calculated using 3 different critical reference central points (MCT and anterior and posterior apices), whereas Ambrosio and associates[18] only used MCT as the center for calculations.

In the current literature, there are several topography-based studies comparing differences between pediatric and adult KC.[19–24] These studies concluded that cone is more centrally located (related to less irregular astigmatism), progression is faster (increase in corneal curvature and stromal thinning), and the need for corneal transplantation is higher in pediatric patients with KC.[4–6,19–23] Another important problem is delay or error in diagnosis of KC in the pediatric age group, and about 28%-30% of the cases have stage 4 KC at the time of diagnosis.[15,19,25] Several factors have been suggested to lead this condition. For instance, the high compensatory capacity of intraocular structures in pediatrics might partially eliminate corneal aberrations and refractive deterioration caused by KC; and preservation of binocular vision until involvement of the dominant eye (since KC is an asymmetrical disease) might delay clinical symptoms and complaints, as well the diagnosis.[6,26–28]

On the other hand, DS is a well-known risk factor for developing KC in the pediatric age group.[1–3] In the current study, a validation analysis was also performed in pediatric DS patients as an "at risk" group to evaluate the ability of morphogeometric and volumetric parameters in detection of early KC, and it was shown that $D_{apexant}$ and V_{total} had highly satisfying sensitivity (100% for both) and specificity (88.2% and 85.3%, respectively) in discrimination of early KC from normal. It should be stated that the recent evidence by Alio and associates demonstrated that DS corneas have specific features, and 71.3% of the DS corneas represented KC-compatible corneal topography.[29,30] Therefore, the differences in morphogeometry between DS and non-DS subjects might have affected our validation analysis in the pediatric DS group in the current study, in which some of the parameters showed insignificant discriminating ability ($D_{apexpost}$, $D_{apexant}$-$D_{apexpost}$ difference, and VOL_{MCTrel}), although they had significant power in the non-DS pediatric KC group.

In conclusion, the current study firstly presented 3-D morphogeometric and volumetric characterization of the cornea in pediatric patients with early and mild KC using a virtual corneal model. It was also demonstrated that pediatric patients with early and mild KC both have decreased corneal thickness and volume; however, posterior apex displacement, difference between anterior and posterior corneal apex deviation, and relative volume increase between 1.0- and 1.4-mm-diameter circles centered on the thinnest corneal point seem to be signs of early KC. These morphogeometric and volumetric parameters can be integrated with ectasia-screening software of the topographer and might assist the clinician in early detection of KC in the pediatric age-group, where prompt treatment is critical.

FUNDING/SUPPORT: THIS STUDY HAS BEEN CARRIED OUT IN THE FRAMEWORK OF THE THEMATIC NETWORK FOR CO-OPERATIVE Research in Health (RETICS) reference number RD16/0008/0012 financed by the Carlos III Health Institute-General Sub-direction of Networks and Cooperative Investigation Centers (R&D&I National Plan 2013-2016) and the European Regional Development Fund (FEDER). Financial Disclosures: Jorge L. Alió del Barrio works as a medical advisor for CSO. The rest of the authors declare no financial or proprietary interest in any product or company associated with any device, instrument, or drug mentioned in this article. All authors attest that they meet the current ICMJE criteria for authorship.

REFERENCES

1. Rabinowitz YS. Keratoconus. *Surv Ophthalmol* 1998;42(4):297–319.
2. Mukhtar S, Ambati BK. Pediatric keratoconus: a review of the literature. *Int Ophthalmol* 2018;38(5):2257–2266.
3. Sabti S, Tappeiner C, Frueh BE. Corneal cross-linking in a 4-year-old child with keratoconus and Down syndrome. *Cornea* 2015;34(9):1157–1160.
4. Chatzis N, Hafezi F. Progression of keratoconus and efficacy of pediatric corneal collagen cross-linking in children and adolescents. *J Refract Surg* 2012;28:753–758.
5. Naderan M, Rajabi MT, Zarrinbakhsh P, Farjadnia M. Is keratoconus more severe in pediatric population? *Int Ophthalmol* 2017;37(5):1169–1173.
6. Olivo-Payne A, Abdala-Figuerola A, Hernandez-Bogantes E, Pedro-Aguilar L, Chan E, Godefrooij D. Optimal management of pediatric keratoconus: challenges and solutions. *Clin Ophthalmol* 2019;13:1183–1191.
7. Cavas-Martinez F, Fernandez-Pacheco DG, De la Cruz-Sanchez E, et al. Geometrical custom modeling of human cornea in vivo and its use for the diagnosis of corneal ectasia. *PloS One* 2014;9(10):e110249.
8. Cavas-Martinez F, Bataille L, Fernandez-Pacheco DG, Canavate FJF, Alio JL. A new approach to keratoconus detection based on corneal morphogeometric analysis. *PLoS One* 2017;12(9):e0184569.
9. Cavas-Martinez F, Bataille L, Fernandez-Pacheco DG, Canavate FJF, Alio JL. Keratoconus detection based on a new corneal volumetric analysis. *Sci Rep* 2017;7(1):15837.
10. Rabinowitz YS, Rasheed K. KISA% index: a quantitative videokeratography algorithm embodying minimal topographic criteria for diagnosing keratoconus. *J Cataract Refract Surg* 1999;25(10):1327–1335.
11. Mas Tur V, MacGregor C, Jayaswal R, O'Brart D, Maycock N. A review of keratoconus: Diagnosis, pathophysiology, and genetics. *Surv Ophthalmol* 2017;62(6):770–783.
12. Alio JL, Pinero DP, Aleson A, et al. Keratoconus-integrated characterization considering anterior corneal aberrations, internal astigmatism, and corneal biomechanics. *J Cataract Refract Surg* 2011;37(3):552–568.
13. Vega-Estrada A, Alio JL. Keratoconus corneal posterior surface characterization according to the degree of visual limitation. *Cornea* 2019;38(6):730–736.
14. Vega-Estrada A, Mimouni M, Espla E, Alio Del Barrio J, Alio JL. Corneal epithelial thickness intrasubject repeatability and its relation with visual limitation in keratoconus. *Am J Ophthalmol* 2019;200:255–262.
15. El-Khoury S, Abdelmassih Y, Hamade A, et al. Pediatric keratoconus in a tertiary referral center: incidence, presentation, risk factors, and treatment. *J Refract Surg* 2016;32(8):534–541.
16. Mazzotta C, Traversi C, Baiocchi S, et al. Corneal collagen cross-linking with riboflavin and ultraviolet A light for pediatric keratoconus: ten-year results. *Cornea* 2018;37(5):560–566.
17. Meek KM, Tuft SJ, Huang Y, et al. Changes in collagen orientation and distribution in keratoconus corneas. *Invest Ophthalmol Vis Sci* 2005;46(6):1948–1956.
18. Ambrosio R Jr, Alonso RS, Luz A, Coca Velarde LG. Corneal-thickness spatial profile and corneal-volume distribution: tomographic indices to detect keratoconus. *J Cataract Refract Surg* 2006;32(11):1851–1859.
19. Leoni-Mesplie S, Mortemousque B, Touboul D, et al. Scalability and severity of keratoconus in children. *Am J Ophthalmol* 2012;154(1):56–62.e51.
20. Buzzonetti L, Valente P, Petrocelli G. Keratoconus in children. In: Alio J, ed. Keratoconus. Cham: Springer; 2017:43–49.
21. Kamiya K, Ishii R, Shimizu K, Igarashi A. Evaluation of corneal elevation, pachymetry and keratometry in keratoconic eyes with respect to the stage of Amsler-Krumeich classification. *Br J Ophthalmol* 2014;98(4):459–463.
22. Kankariya VP, Kymionis GD, Diakonis VF, Yoo SH. Management of pediatric keratoconus - evolving role of corneal collagen cross-linking: an update. *Indian J Ophthalmol* 2013;61(8):435–440.
23. Soeters N, van der Valk R, Tahzib NG. Corneal cross-linking for treatment of progressive keratoconus in various age groups. *J Refract Surg* 2014;30(7):454–460.
24. Toprak I, Yaylali V. Comparison of anterior segment parameters between pediatric and adult keratoconus groups. *Ege J Med* 2018;57:19–25.
25. Arora R, Lohchab M. Pediatric keratoconus misdiagnosed as meridional amblyopia. *Indian J Ophthalmol* 2019;67(4):551–552.
26. Schlegel Z, Lteif Y, Bains HS, Gatinel D. Total, corneal, and internal ocular optical aberrations in patients with keratoconus. *J Refract Surg* 2009;25(10 Suppl):S951–S957.
27. Sahebjada S, Fenwick EK, Xie J, Snibson GR, Daniell MD, Baird PN. Impact of keratoconus in the better eye and the worse eye on vision-related quality of life. *Invest Ophthalmol Vis Sci* 2014;55(1):412–416.
28. Al Suhaibani AH, Al-Rajhi AA, Al-Motowa S, Wagoner MD. Inverse relationship between age and severity and sequelae of acute corneal hydrops associated with keratoconus. *Br J Ophthalmol* 2007;91(7):984–985.
29. Alio JL, Vega-Estrada A, Sanz P, et al. Corneal morphologic characteristics in patients with Down syndrome. *JAMA Ophthalmol* 2018;136(9):971–978.
30. Vega-Estrada A, Fariselli C, Alio JL. Posterior corneal features in patients with down syndrome and their relation with keratoconus. *Br J Ophthalmol* 2020; https://doi.org/10.1136/bjophthalmol-2019-314939. In press.